

# INFLUENCE OF VOLUME FRACTION, SIZE, CRACKING, CLUSTERING OF PARTICULATES AND POROSITY ON THE STRENGTH AND STIFFNESS OF 6063/SiC<sub>p</sub> METAL MATRIX COMPOSITES

A. Chennakesava Reddy<sup>1</sup>

<sup>1</sup>Professor, Department of Mechanical Engineering, JNTUH College of Engineering, Kukatpally, Hyderabad – 500 085, Telangana, India

## Abstract

The objective of this study is to examine the influence of volume fraction, size of particulates, formation of precipitates at the matrix/particle interface, particle cracking, voids/porosity, and clustering of particulates on the strength and stiffness of 6063/SiC<sub>p</sub> metal matrix composites. Tensile strength and stiffness increase with an increase in the volume fraction of SiC particulates. The tensile strength and stiffness decrease with increase in size of the particulates, presence of porosity, clustering, and particle cracking. Formation of particulate clusters is more prominent in the composites having very small-reinforced particulates. Mg<sub>2</sub>Si compound is likely to precipitate at the matrix/particle interfaces of 6063/SiC composite.

**Keywords:** 6063, SiC, clustering, cracking, porosity, clustering

\*\*\*

## 1. INTRODUCTION

Consolidation of a high strength ceramic particulate in a soft metal matrix is the technological renovation in the domain of composites for the designer to assure high specific elastic modulus, strength-to-weight ratio, fatigue durability, and wear resistance in the fields of aerospace and automotive applications. In cast metal-matrix composites, particle clustering is unavoidable because of the pooled effect of particulate sedimentation and refusal of the particulate by the matrix dendrites during solidification [1-8]. An additional possibility of particle clustering is very common with small particulates in the metal matrix composites. The potential reason for the failure of aluminium-silicon carbide composites at low tensile strains involves the formation of voids by the interfacial debonding [9]. The porosity in the composite reduces its strength. The possibility of porosity in the composites is because of entrapped gases during casting. Because of tensile loading, the metal matrix is subjected to tensile stress while the reinforced particulates undergo compressive stress this contributes to particulate cracking. Particulates must be uniformly dispersed in order to achieve good wetting. This is generally achieved by mechanical agitation. A two-step stir casting process has been extensively studied and is well known [10]. The precipitate that forms during solidification may influence strengthening mechanism in the composite [11]. Silicon carbide (SiC) reacts with molten aluminum at temperatures above 1000 K to form Al<sub>4</sub>C<sub>3</sub>, releasing silicon into the matrix. The brittle precipitate Al<sub>4</sub>C<sub>3</sub> condenses the strength of composite. All these phenomena may influence the tensile strength and stiffness of composite.

The understanding and control of the underlying metallurgical phenomena while manufacturing the metal

matrix composite have become of principal importance for the manufacturer to make a quality product as per the designer specifications. The objective of this work is to study the influence of the volume fraction and particle size of SiC<sub>p</sub>, clustering and cracking of particulates, voids/porosity, and formation of precipitates at the particle/matrix interface on the tensile strength and stiffness of 6063/SiC<sub>p</sub> metal matrix composites. The wettability of SiC particulates is secured through the following methods:

- Preheating of SiC particulates before adding into the molten metal
- Two-stage stirring of molten metal and SiC particulates
- Adding of Mg to the molten metal
- Filling the die with compressed argon gas.

## 2. WEIBULL MODEL

The Weibull cumulative distribution to find reliable strength of composite is presented by:

$$F(x) = 1 - \exp\left(-\left(\frac{x}{\alpha}\right)^\beta\right) \quad (1)$$

$$\ln\left[\ln\left(\frac{1}{1-F(x)}\right)\right] = \beta \ln x - \beta \ln \alpha = mx + c \quad (2)$$

where  $m$  is the slope of a straight line and  $c$  is the intercept. So, when we perform the linear regression, the shape parameter ( $\beta$ ) comes directly from the slope of the line. The scale parameter ( $\alpha$ ) must be calculated as follows:

$$\alpha = \exp(-c/\beta) \quad (3)$$

According to the Weibull statistical-strength theory for brittle materials, the probability of survival,  $P$  at a maximum stress ( $\sigma$ ) for uniaxial stress field in a homogeneous material governed by a volumetric flaw distribution is given by

$$P(\sigma_f \geq \sigma) = R(\sigma) = \exp(-B(\sigma)) \quad (4)$$

where  $\sigma_f$  is the value of maximum stress of failure,  $R$  is the reliability, and  $\beta$  is the risk of rupture. For a two-parameter Weibull model, the risk of rupture is of the form

$$B(s) = A \left( \sigma_f / \sigma_0 \right)^\beta \quad (\sigma_0, \beta > 0) \quad (5)$$

where  $\sigma_0$  is the characteristic strength, and  $\beta$  is the shape factor, which characterizes the flaw distribution in the material. Both of these parameters are considered material properties independent of specimen size. The author has proposed expression for the tensile strength considering the effects of reinforced particle size and porosity. The expression of tensile strength is presented below:

$$\sigma_t = \sigma_o [V_m + V_p - V_v]^{1/\beta} \quad (\sigma_o, \beta_t > 0) \quad (6)$$

where  $V_m$ ,  $V_p$ , and  $V_v$  are respectively volume of the matrix, volume of the reinforced particles and volume of the porosity in the tensile specimen.

### 3. MATERIALS AND METHODS

The matrix alloy was 6063 matrix. The reinforcement was silicon carbide particulates ( $\text{SiC}_p$ ) particulates. The volume fractions of  $\text{SiC}_p$  reinforcement are 12%, 16%, and 20%. The particle sizes of  $\text{SiC}_p$  reinforcement are 800 nm, 10  $\mu\text{m}$ , and 20  $\mu\text{m}$ .

#### 3.1 Preparation of Metal Matrix Composites

The 6063 aluminium alloy matrix was melted in a resistance furnace. A graphite crucible was used to melt the metal. The 6063 was cut into little pieces and place into the crucible to form a bottom layer of the ground substance. The melting losses of the alloy constituents were involved into account while fixing the complaint. Then SiC particles (as per volume fraction required in the composite) were carefully laid on top of this layer mitigating the drop of particles to the underside of the crucible. After that, other pieces of 6063 were placed above the particles to ensure scattering of the particles in the bulk. The whole crucible was then heated. During the melting process, the charge was fluxed with coverall to prevent dressing. The molten alloy was degasified by tetrachlorethane (in solid shape). The crucible was taken off from the furnace and treated with sodium modifier. Then the liquid melt was allowed to cool down

just below the liquidus temperature to get the melt semi solid state. At this stage, the preheated (500°C for 1 hour) SiC particles were added to the liquid melt. The molten alloy and SiC particles are thoroughly stirred manually for 15 minutes. After manual steering, the semisolid liquid melt was reheated to a full liquid state in the resistance furnace followed by an automatic mechanical stirring using a mixer to make the melt homogenous for about 10 minutes at 200 rpm. The temperature of melted metal was measured using a dip type thermocouple. The preheated cast iron die was filled with dross-removed melt by the compressed (3.0 bar) argon gas [10].

#### 3.2 Heat Treatment

Prior to the machining of composite samples, a solution treatment was applied at 500°C for 1 hour, followed by quenching in cold water. The samples were then naturally aged at room temperature for 100 hours.

#### 3.3 Tensile Tests

The heat-treated samples were machined to get flat-rectangular specimens (Fig.1) for the tensile tests. The tensile specimens were placed in the grips of a Universal Test Machine (UTM) at a specified grip separation and pulled until failure as shown in Fig.2. The test speed was 2 mm/min (as for ASTM D3039). The load v/s displacement curve was obtained from the computer interfaced with the UTM.

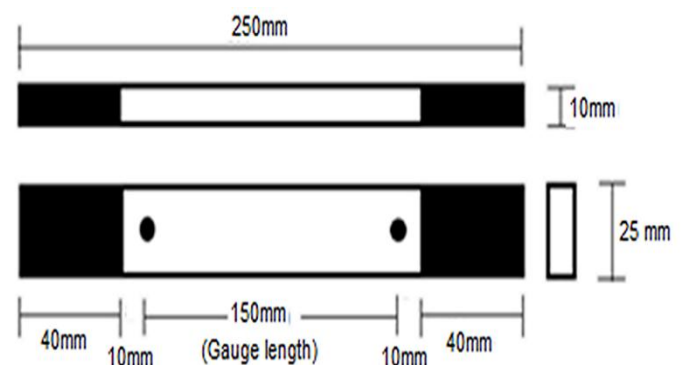


Fig – 1: Dimensions of flat tensile specimen

#### 3.4 Optical and Scanning Electron Microscopic Analysis

An image analyzer was used to study the distribution of the reinforcement particles within the 6063 aluminum alloy matrix. The polished specimens were ringed with distilled water and were etched with 0.5% HF solution for optical microscopic analysis. Fracture surfaces of the deformed/fractured test samples were analyzed with a scanning electron microscope (S-3000N Toshiba SEM) to define the macroscopic fracture mode and to establish the microscopic mechanisms governing fracture.



Fig – 2: Tensile testing of metal matrix composite

#### 4. RESULTS AND DISCUSSION

The stiffness is the elasticity modulus of the composite. The tensile failure may be either cross-section failure of the workpiece or degradation of the composite at a microscopic scale. The tensile strength is the maximum stress that the material can sustain under a uniaxial loading. The influence of characteristic parameters on the strength, stiffness, and reliability of 6063/SiC particulate metal matrix composite are discussed in the following sections.

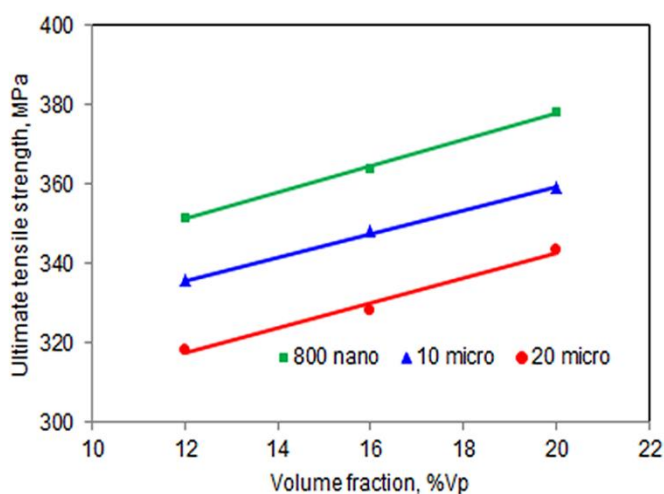


Fig – 3: Variation of the tensile strength with the volume fraction and particle size of SiCp

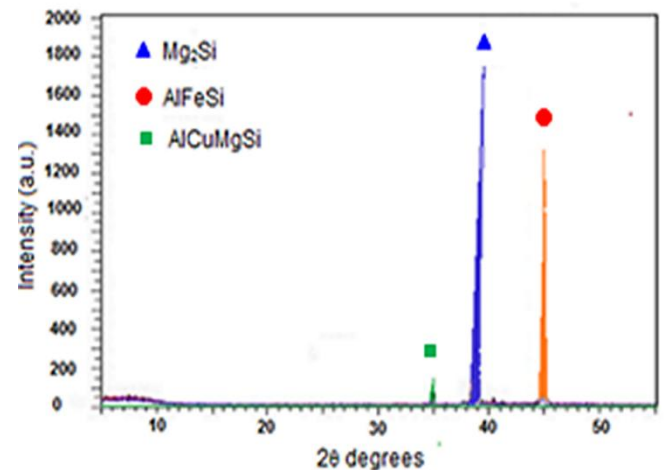


Fig – 4: EDS analysis of heat-treated 6063/SiC metal matrix composite (particle size = 20 $\mu$ m; vp = 20%).

#### 4.1 Dynamics of Strengthening Mechanism in 6063/SiC Composite

The influence of volume fraction and particle size on tensile strength with is presented in Fig.3. It is evidently displayed that, for a given particle size the tensile strength increases with an increase in the volume fraction of SiCp. As the particle size increases the tensile strength decreases. The strengthening mechanism in the particulate dispersed metal matrix composite is because of obstruction to the movement of dislocations and the deformation of material [12, 13]. The amount of obstruction to the dislocations is high for small particles. It has been mentioned that the work hardening rate increases with increasing volume fraction of reinforcement [14]. The other possibility, of increasing strength is owing to the formation of precipitates at the particle/matrix interface and enhancement of wettability. The driving force for wetting is affected by only two factors: surface tension of the liquid and the strength of the solid-liquid interaction at the interface, which leads to a reduced interface tension [15]. The presence of Mg increases the surface tension, which subsequently enhances the wettability. The two-stage stirring also offers a better matrix-particle bonding due to stirring action of particles into the melt. The formation of  $Al_4C_3$  can be avoided by minimizing the contact time of SiC with the melt [16]. The two-stage stirring and fast filling of the die cavity under pressurized argon gas avoid the formation of  $Al_4C_3$ . The formation of precipitates can be observed in the EDS graph shown in Fig.4. The other strengthening precipitates are AlFeSi and AlCuMgSi. Fig.5 shows the needle-like  $Mg_2Si$  precipitate in the 6063/SiC composite. The precipitation hardening also influences the direct strengthening of the composite due to heat treatment. The 6063/SiC derives its strength from  $Mg_2Si$  precipitates.

#### 4.2 Catastrophe of Strengthening Mechanism in 6063/SiC Composite

The coarse particles are more probable to contain flaws, which may severely reduce their strength than smaller particles [17, 18]. Non-planar cracking of particle (Fig.6a) is

observed in the 6063/SiCp composite comprising 20µm particles. For composite of 20% volume fraction and 800 nm, the tensile strength was 378.2 MPa. For composite of 20% volume fraction and 20 µm, the tensile strength was 343.6 MPa. This is the situation of nano particle composite versus micro particle composite. The decrease in tensile strength was 34.6 MPa. This is because of the low passion's ratio (0.14) of SiC particle as than that (0.33) of 6063. The SiC particle experiences compressive stress in the transverse direction of tensile loading.

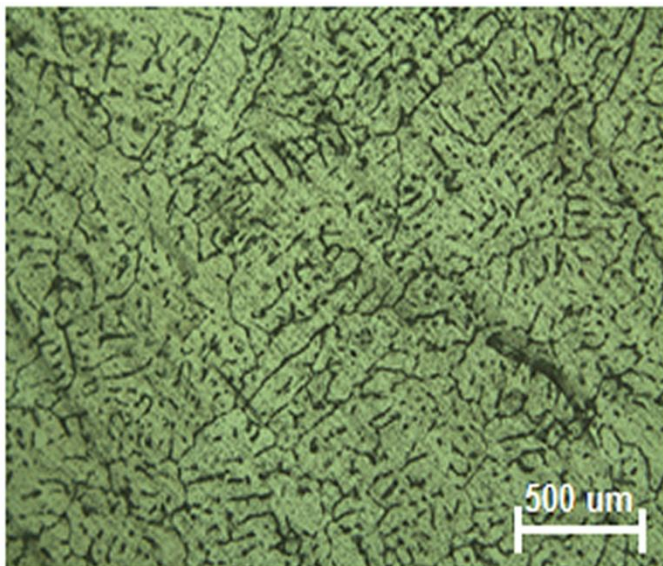


Fig – 5: Formation of precipitates in 6063/SiC composite (particle size = 10µm; vp = 20%).

There is every possibility of cavity formation during the preparation of composite or during testing of composite due to debonding [19]. The porosity of approximately 42µm is also revealed in the 6063/SiCp composite having 20µm particles as shown in Fig.6b. There is a possibility of clustering of SiC particles. These clusters act as sites of stress concentration. The formation of clustering increases with an increase in the volume fraction and with a decrease in the particle size. The remained slurry of melt and particulates was gravity poured into an open metal die. The solidified sample was tested for sedimentation and clustering. Closed packed clusters of smaller particles are observed in the leftover composite material as shown in Fig.7. Even though the two-stage stirring and the addition of Mg are adopted, still there is sedimentation of SiC particles in the crucible. This is where further research is needed for the application of casting route to cast nano particulate metal matrix composites.

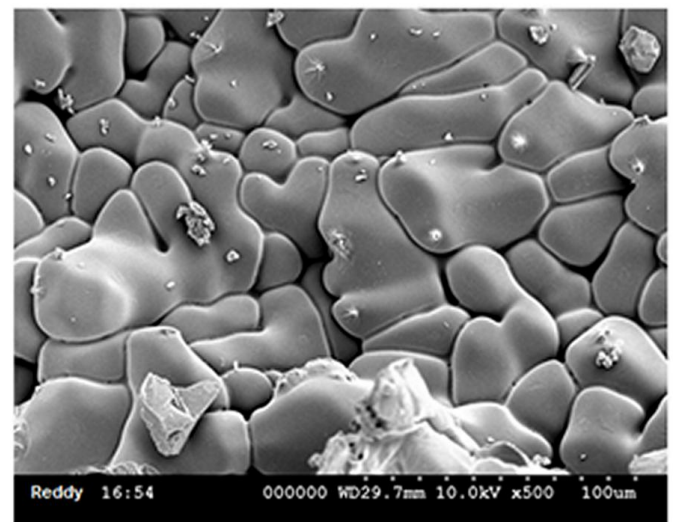


Fig – 7: Clustering of 800 nano particles

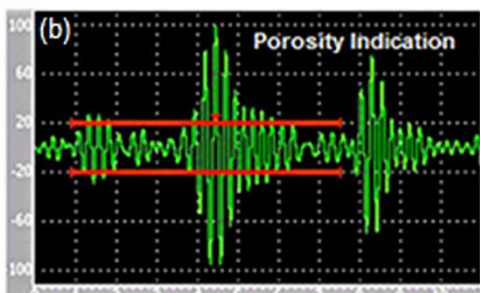
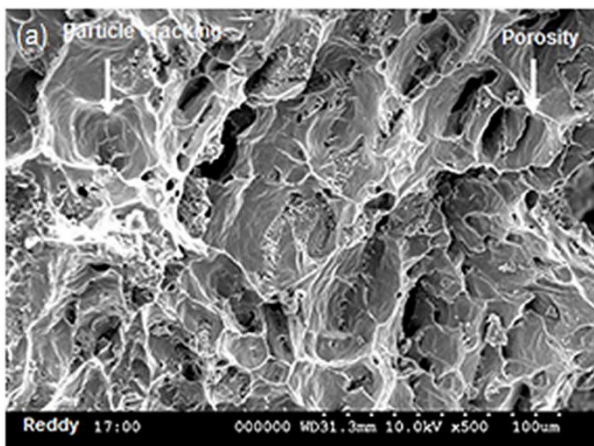


Fig – 6: Particle cracking and porosity (particle size 20 µm, vp =20%)

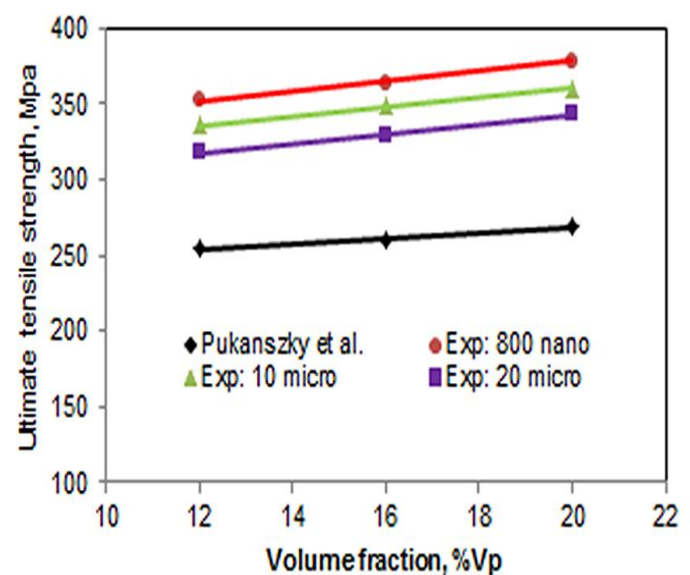


Fig – 8: Comparison of Pukanszky et al criterion with experimental values

### 4.3 Theories of Strengthening Mechanisms

The strength of a particulate composite depends on the strength of the weakest zone and metallurgical phenomena in it. Pukanszky et al [20] presented an empirical relationship for very strong particle-matrix interfacial bonding, as given below:

$$\sigma_c = \left[ \sigma_m \left( \frac{1 - v_p}{1 + 2.5v_p} \right) \right] e^{Bv_p} \tag{7}$$

where  $B$  is an empirical constant, which depends on the surface area of particles, particle density and interfacial bonding energy. The value of  $B$  varies between from 3.49 to 3.87. This criterion has taken care of the presence of particulates in the composite and interfacial bonding between the particle/matrix. The trend of variation of tensile strength is same as experimental results as shown in Fig.8. Nevertheless, the issue of particle size and voids/porosity were not studied in this standard.

An empirical linear relationship between composite strength and particle size was proposed by Landon et al [21]:

$$\sigma_c = \sigma_m(1 - v_p) - k(v_p)d_p \tag{8}$$

where  $k(v_p)$  is the gradient of the tensile strength against the mean particle size (diameter) and is a function of particle volume fraction  $v_p$ . This criterion is applicable to poorly bonded micro-molecules, but cannot apply to strong interfacial adhesion. The tensile strength decreases with an increase in the volume fraction. This criterion does not follow the trend of the experimental results as shown in Fig.9.

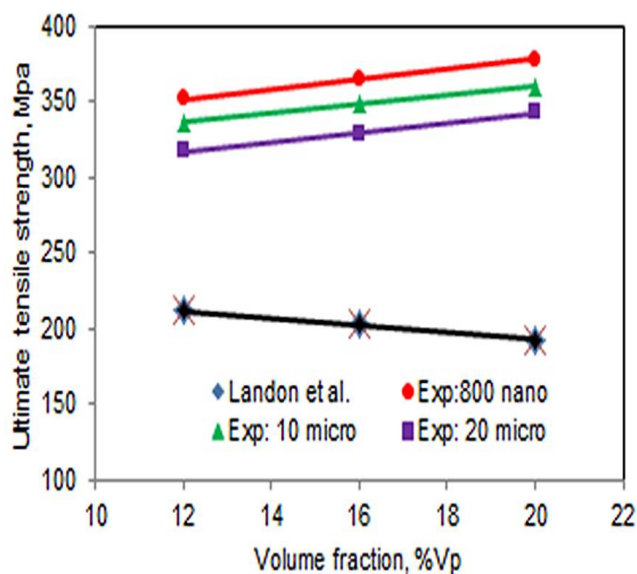


Fig-9: Comparison of Landon et al criterion with experimental values

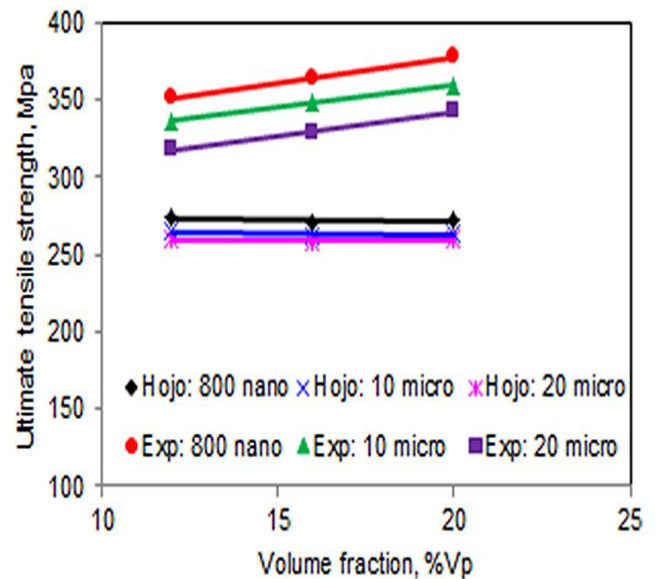


Fig-10: Comparison of Hojo criterion with experimental values

Hojo et al. [22] found that the strength of a composite varies linearly with the mean particle size  $d_p$  according to the relation

$$\sigma_c = \sigma_m + k(v_p)d_p^{-1/2} \tag{9}$$

where  $k(v_p)$  is a constant being a function of the particle loading. This criterion fails for larger particles as shown in Fig.10. However, the composite strength decreases with increasing filler loading in the composite.

A new criterion is suggested by the author considering adhesion, formation of precipitates, particle size, agglomeration, voids/porosity, obstacles to the dislocation, and the interfacial reaction of the particle/matrix. The formula for the strength of composite is stated below:

$$\sigma_c = \left[ \sigma_m \left( \frac{1 - (v_p + v_v)^{2/3}}{1 - 2(v_p + v_v)} \right) \right] e^{m_m(v_p + v_v)} + k(v_p)m_p d_p^{-1/2} \tag{10}$$

where  $v_v$  is the volume fraction of voids/porosity in the composite,  $m_m$  and  $m_p$  are the poisson's ratios of the matrix and particulates, and  $k(v_p)$  is the slope of the tensile strength against the mean particle size (diameter) and is a function of particle volume fraction  $v_p$ . The computed tensile strength values are within the permissible bounds of the experimental results as shown in Fig.11.

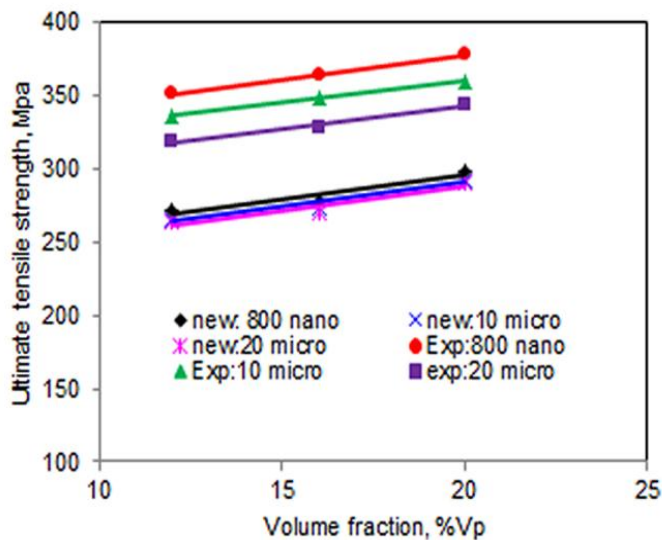


Fig -11: Comparison of the proposed criterion with experimental values

4.4 Elastic Modulus

Elastic modulus is a measure of the stiffness of a material. Anisotropy prevails in many composites. Silicon carbide (SiC) is much stiffer than 6063 aluminium alloy. Kerner [23] found equation for estimating the modulus of a composite that contains spherical particles in a matrix as follows:

$$E_c = E_m \left( 1 + \frac{v_p}{1 - v_p} \frac{15(1 - m_m)}{8 - 10m_m} \right) \tag{11}$$

for  $E_p \geq E_m$  and  $m_m$  is the matrix poisson's ratio.  $V_p$  is the volume fraction;  $E_m$  is the elastic modulus of the matrix.

Counto [24] proposed a simple model for a two phase particulate composite by assuming perfect bonding between particle and matrix. The elastic modulus of the composite is given by

$$\frac{1}{E_c} = \frac{1 - v_p^{1/2}}{E_m} + \frac{1}{(1 - v_p^{1/2})v_p^{1/2}E_m + E_p} \tag{12}$$

where  $v_p$  is the elastic modulus of SiCp.

Ishai and Cohen [25] developed based on a uniform stress applied at the boundary, the elastic modulus of the composite is given by

$$\frac{E_c}{E_m} = 1 + \frac{1 + (\delta - 1)v_p^{2/3}}{1 + (\delta - 1)(v_p^{2/3} - v_p)} \tag{13}$$

which is upper-bound equation. They assumed that the particle and matrix are in a state of macroscopically homogeneous and adhesion is perfect at the interface. The lower-bound equation is given by

$$\frac{E_c}{E_m} = 1 + \frac{v_p}{\delta / (\delta - 1) - v_p^{1/3}} \tag{14}$$

where  $\delta = E_p / E_m$ .

The Young's modulus of particulate composites with the modified rule of mixtures [26] is given by:

$$E_c = \chi_p E_p v_p + E_m (1 - v_p) \tag{15}$$

Where  $0 < \chi_p < 1$  is a particulate strengthening factor.

The proposed equation by author to find elastic modulus includes the effect of voids/porosity in the composite as given below:

$$\frac{E_c}{E_m} = \left( \frac{1 - v_v^{2/3}}{1 - v_v^{2/3} + v_v} \right) + \left( \frac{1 + (\delta - 1)v_p^{2/3}}{1 + (\delta - 1)(v_p^{2/3} - v_p)} \right) \tag{16}$$

where  $v_v$  is the volume fraction of voids/porosity in the composite. The elastic moduli computed from the above criteria are registered in Table 1. The values of elastic moduli obtained from the proposed expression are nearly equal to those of Ishai and Cohen criteria.

Table 1 Elastic modulus obtained from various criteria

Criteria	Young's modulus, GPa		
	Vp =12	Vp =16	Vp =20
Kerner	83.11	88.71	94.86
Counto	105.57	115.00	124.82
Ishai and Cohen (upper bound)	163.43	170.75	178.08
Ishai and Cohen (lower bound)	80.68	85.74	91.35
Rule of mixture (modified)	85.32	90.76	96.2
New proposal by Authors	162.025	168.87	175.72

4.5 Weibull Statistical Strength Criterion

The tensile strength of 6063/SiCp was analyzed by Weibull statistical strength criterion using Microsoft Excel software. The 6063/SiCp composite indicates increasing failure rate ( $\beta$  values much higher than 1.0). The Weibull graphs of tensile strength indicate lesser reliability for volume fractions of 12% than those reliabilities of 16%, and 20% (Fig.12). The shape parameters,  $\beta_s$  (gradients of graphs) are 22.36, 22.71, and 21.40 respectively, for the composites having the particle volume fraction of 12%, 16%, and 20%.

The Weibull characteristic strength is a measure of the scale in the distribution of data. It is so happened that  $\sigma_0$  equals the strength at which 63.2 percent of the composite has failed. With 6063/SiCp, about 36.8 percent of the tensile

specimens should survive at least 342.40 MPa, 354.22 MPa, and 367.03 MPa for 12%, 16%, and 20% volume fractions of SiCp in the specimens respectively. The reliability graphs of tensile strength are shown in figure 13. At reliability 0.90 the survival tensile strength of 6063/SiCp containing 12% of volume fraction is 309.61 MPa, 16% of volume fraction is 320.80 MPa, and 20% of volume fraction is 330.39 MPa.

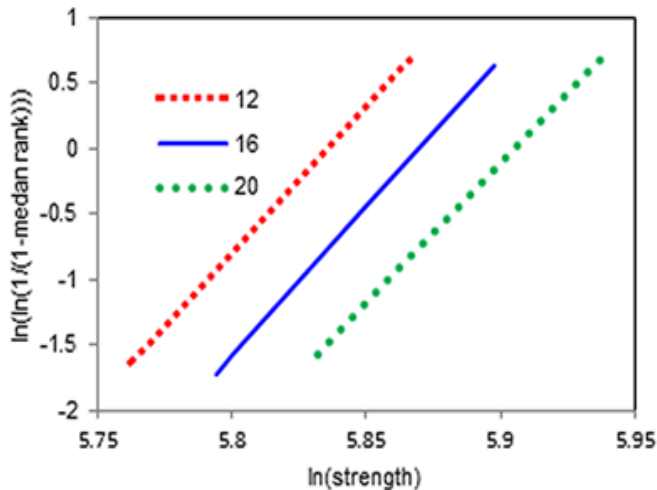


Fig -12: Weibull distribution of tensile strength

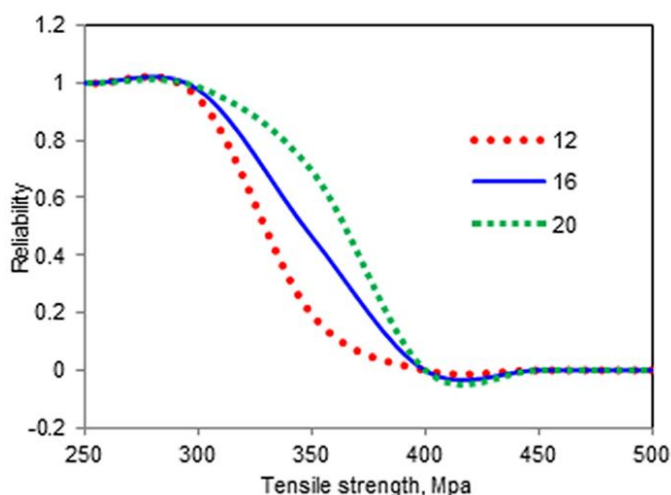


Fig -13: Reliability graphs for tensile strength of 6063/SiCp

#### 4.6 Fracture

The failure path in these composites is from the matrix through the matrix/particle interface to the particles. The cracking of SiC particles is a rare event for small size ( $\leq 10\mu\text{m}$ ) of particles [27-29]. The ductile and ductile-brittle fracture is observed in the composite consisting of 20% volume fraction and 800 nm particle size of SiC as shown in Fig. 14a. The clustering is also observed in this composite. The reason may be the presence of small size SiC reinforcement particles reduces the average distance in the composite to form clustering and to act as strong barriers to dislocation motion. The ductile-brittle and brittle fracture is observed in the composite consisting of 16% volume fraction and 10  $\mu\text{m}$  particle size of SiC as shown in Fig. 14b. The porosity is observed in the composite having 20 $\mu\text{m}$  size

of particulates as shown in Fig.14c. The presence of voids is also observed in the composites having larger SiCp particles. The fracture mode is brittle. The void coalescence occurs when the void elongates to the initial intervoid spacing. The dimpled appearance of the fractured surfaces is observed in all the composites.

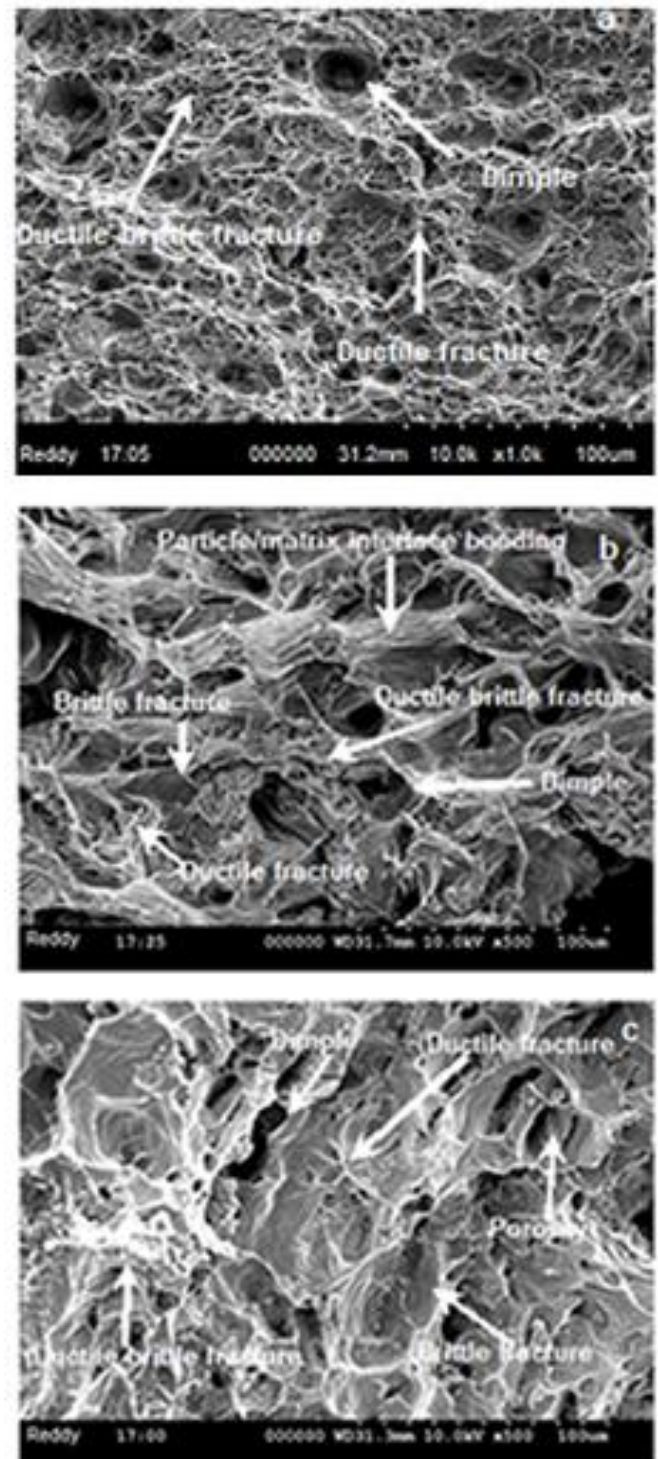


Fig - 14: SEM of fracture surface of 6063/SiC composites (a) of 20% Vp and 800 nm particle size (b) of 16% Vp and 10  $\mu\text{m}$  particle size (c) of 20% Vp and 20 $\mu\text{m}$  particle size.

## 5. CONCLUSION

The EDS report confirms the presence of  $Mg_2Si$  precipitates in the 6063/SiC<sub>p</sub> composites. The porosity of approximately 42 $\mu$ m was observed in the 6063/SiC<sub>p</sub> composite having 20 $\mu$ m particles. At higher volume fractions and small size particles, the particle-particle interaction may develop clustering in the composite. Non-planar cracking of particle was observed in the 6063/SiC<sub>p</sub> composite comprising 20 $\mu$ m particles. The tensile strength increases with increase in volume fraction of SiC<sub>p</sub>, whereas it decreases with increasing particle size. The fracture mode was ductile-brittle in nature.

## REFERENCES

- [1]. D.J.Lloyd, Particle reinforced aluminum and magnesium matrix composites, *International Material Reviews*, 39, (1994), 1-23.
- [2]. A. C. Reddy, Mechanical properties and fracture behavior of 6061/SiC<sub>p</sub> Metal Matrix Composites Fabricated by Low Pressure Die Casting Process, *Journal of Manufacturing Technology Research*, 1(2009), 273-286.
- [3]. A. C.Reddy, Essa Zitoun, Tensile behavior Of 6063/Al<sub>2</sub>O<sub>3</sub> particulate metal matrix composites fabricated by investment casting process, *International Journal of Applied Engineering Research*, 1, (2010), 542-552.
- [4]. A. C. Reddy, Essa Zitoun, Tensile properties and fracture behavior of 6061/Al<sub>2</sub>O<sub>3</sub> metal matrix composites fabricated by low pressure die casting process, *International Journal of Materials Sciences*, 06, (2011), 147-157.
- [5]. A. Chennakesava Reddy, Strengthening mechanisms and fracture behavior of 7072Al/Al<sub>2</sub>O<sub>3</sub> metal matrix composites, *International Journal of Engineering Science and Technology*, 03, (2011), 6090-6100.
- [6]. A. C. Reddy, Evaluation of mechanical behavior of Al-alloy/Al<sub>2</sub>O<sub>3</sub> metal matrix composites with respect to their constituents using Taguchi , *International Journal of Emerging Technologies and Applications in Engineering Technology and Sciences*, 04, (2011), 26-30.
- [7]. A. Chennakesava Reddy, Tensile fracture behavior of 7072/SiC<sub>p</sub> metal matrix composites fabricated by gravity die casting process, *Materials Technology: Advanced Performance Materials*, 26, (2011), 257-262.
- [8]. A. C. Reddy , Evaluation of mechanical behavior of Al-alloy/SiC metal matrix composites with respect to their constituents using Taguchi techniques, *i-manager's Journal of Mechanical Engineering*, 01, (2011), 31-41.
- [9]. S.R. Nutt, J.M.Duva, A failure mechanism in Al-SiC composites, *Scripta Materialia*, 20, (1986), 1055-1058.
- [10]. A.C.Reddy, and Z.Essa, Matrix Al-alloys for alumina particle reinforced metal matrix composites, *Indian Foundry Journal*, 55, (2009), 12-16.
- [11]. J.C.Lee, K.N.Subramanian, Y.Kim, The interface in Al<sub>2</sub>O<sub>3</sub> particulate-reinforced aluminium alloy composite and its role on the tensile Properties, *Journal of Materials Science*, 29, (1994), 1983-1990.
- [12]. R.J. Arsenault, Relationship between strengthening mechanisms and fracture toughness of discontinuous SiC/Al composites, *Journal of Composites Technology and Research*, 10, (1988), 140-145.
- [13]. A. Chennakesava Reddy, Influence of strain rate and temperature on superplastic behavior of sinter forged Al6061/SiC metal matrix composites, *International Journal of Engineering Research & Technology*, 0974-3154, 04, 02, 189-198, 2011.
- [14]. N. Chawla, Y.L. Shen, Mechanical behavior of particle reinforced metal matrix composites, *Advanced Engineering Materials*, 3, (2001), 357-370.
- [15]. R. Asthana, An empirical correlation between contact angles and surface tension in some ceramic-metal systems, *Metallurgical Transactions A*, 25A, (1994), 225-229.
- [16]. S. Vaucher, O. Beffort, Bonding and interface formation in metal matrix composites, *MMC-Assess – Thematic Network, MMC-Assess Consortium*, 2001, 1-41.
- [17]. M.L.Seleznev, J.A.Cornie, R.P.Mason, M.A.Ryals, Effect of composition, particle size, and heat treatment on the mechanical properties of Al-4.5 wt. % Cu based alumina particulate reinforced composites, *Proceedings of SAE International Congress and Exposition*, Detroit, MI, 1998, P. No. 980700.
- [18]. D.J. Lloyd, Aspects of particle fracture in particulate reinforced MMCs, *Acta Materialia*, 39, (1991), 59-72.
- [19]. A.F. Whitehouse, T.W. Clyne, Cavity formation during tensile straining of particulate and short fiber metal matrix composites, *Acta Materialia*, 41, (1993), 1701-1711.
- [20]. B. Punkanszky, B. Turcsanyi, F. Tudos, Interfaces in polymer, ceramic and metal matrix composites (Edited by Ishida H, Amsterdam, Elsevier, 1988), 467-477.
- [21]. G. Landon, G. Lewis, G. Boden, The influence of particle size on the tensile strength of particulate-filled polymers, *Journal of materials Science*, 12, (1977), 1605-1613.
- [22]. H. Hojo, W. Toyoshima, M. Tamura, N. Kawamura, Short- and long- term strength characteristics of particulate-filled cast epoxy resin, *Polymer Engineering & Science*, 14, (1974), 604-609.
- [23]. E.H. Kerner, The elastic and thermoelastic properties of composite media, *Proceedings of the Physical Society B*, 69, (1956), 808-813.
- [24]. U.J. Counto, Effect of the elastic modulus, creep and creep recovery of concrete, *Magazine of Concrete Research*, 16, (1964), 129-138.
- [25]. O. Ishai, I.J. Cohen, Elastic properties of filled and porous epoxy composites, *International Journal of Mechanical Sciences*, 9, (1967), 539-546.
- [26]. S.Y.Fu, G. Xu, T.W. Mai, On the elastic modulus of hybrid, particle/short fiber/polymer composites, *Composite Part B*, 33, (2002), 291-299.
- [27]. Y. Sugimura, S. Suresh, Effects of SiC content on fatigue crack growth in aluminium alloy reinforced with SiC particles, *Metallurgical Transactions*, 23A, (1992), 2231-2342.
- [28]. A.C. Reddy, Influence of ageing, inclusions and voids on ductile fracture mechanism in commercial Al-alloys, *Indian Journal of Engineering & Material Sciences*, 5, (2002), 365-368.
- [29]. A.C.Reddy, Fracture behavior of brittle matrix and alumina trihydrate particulate composites, *Indian Journal of Engineering & Materials Sciences*, 5, (2002), 365-368.

**BIOGRAPHY**

Dr. A. Chennakesava Reddy, B.E., M.E(prod), M.Tech(CAD/CAM)., Ph.D (prod)., Ph.D (CAD/CAM) is a Professor in Mechanical Engineering, Jawaharlal Nehru Technological University, Hyderabad. The author has published 209 technical papers worldwide. He is the recipient of best paper awards nine times. He is also recipient of Best Teacher Award from the Telangana State, India. He has successfully completed several R&D and consultancy projects. He has guided 14 Research Scholars for their Ph.D. He is a Governing Body Member for several Engineering Colleges in Telangana. He is also editorial member of Journal of Manufacturing Engineering. He is author of books namely: FEA, Computer Graphics, CAD/CAM, Fuzzy Logic and Neural Networks, and Instrumentation and Controls. Number of citations are 325. The total impact factors are 48.250. His research interests include Fuzzy Logic, Neural Networks, Genetic Algorithms, Finite Element Methods, CAD/CAM, Robotics and Characterization of Composite Materials and Manufacturing Technologies.